# Electromagnetic Profiler for Inspections of Steel through Corrosion Product

Paul CROUZEN, Shell Global Solutions International B.V., Amsterdam, The Netherlands
Martin VERWEIJ and Christiaan EGGINK, Delft University of Technology, Delft, The Netherlands

**Abstract**. A novel method is described to assess external corrosion damage of steel by using an electromagnetic profiler with pulsed magnetic fields. This Pulsed Eddy Current (PEC) method has proven to be suited to determine wall loss through thick layers of corrosion products (iron oxides). The paper will show how the measurements can distinguish between steel and corrosion products. The method will be illustrated with an assessment of corrosion damage resulting from Corrosion under Insulation (CUI). Finite element calculations are described that model PEC profiling of steel with cylindrical wall loss defects.

## Introduction

External corrosion is a well-known and often costly threat to the integrity of steel structures and pressure vessels in the oil- and petrochemical industry. Steel is usually protected from corrosion by a paint coating, but this may break down due to mechanical damage or ageing. Once the coating has failed, the steel surface is exposed to air and humidity and starts to corrode. Figure 1 displays an example of a pipe with external corrosion attack. This particular example was the result of 'Corrosion under Insulation' (CUI), which is a corrosion phenomenon highly relevant to the process industry. The corrosion occurred while the pipe was insulated; the picture was taken after the insulation was removed.

Following the discovery of corrosion damage, the asset owner must decide if it is safe to continue operating. For pressurised a pipe it is preferable to take the pipe out of service, depressurise the system, and then remove the corrosion product that has accumulated on the exposed surface. Once the corrosion product has been removed, the remaining steel thickness can be assessed with ultrasound or a pit gauge. Sometimes, however, there is an incentive to keep the equipment in service for a period of time before the corrosion damage is addressed. Safety considerations, however, forbid removal of corrosion product from pressurized equipment, as this may trigger a leak. In such cases, non-destructive methods are required that can quantify remaining steel thickness underneath the corrosion product. Profile radiography is suited for this purpose, but is only applicable for piping with a diameter less than about 10". Piping with a larger diameter and e.g. pressure vessels requires other methods. In this paper we will explore one such method, Pulsed Eddy Current (PEC) profiling [1].

**Figure 1.** Picture of a steel pipe with external corrosion damage resulting from 'Corrosion under Insulation' (CUI)

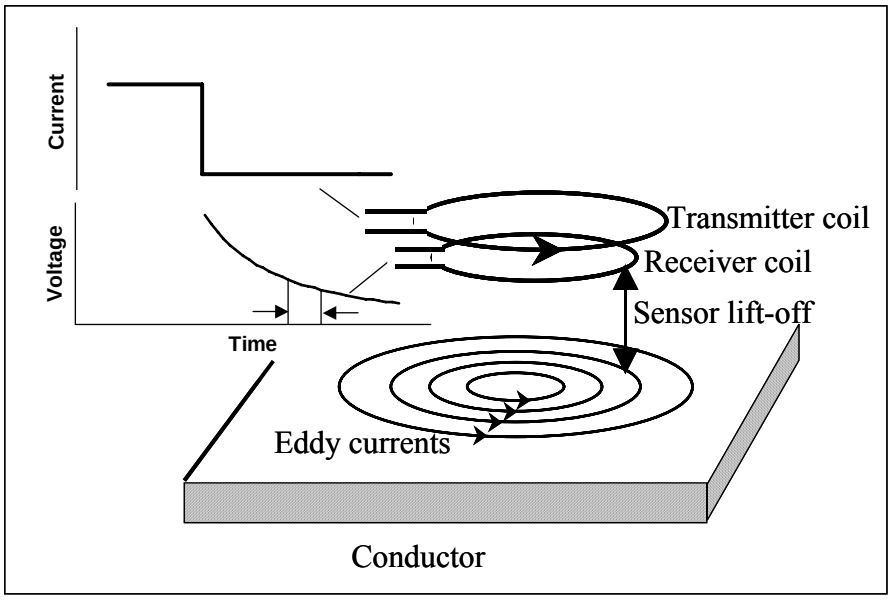


**Figure 2.** Principle of PEC profiling: Eddy currents are induced in a conductor by a pulsed electrical current in a transmission coil. The PEC signal is the voltage induced by the magnetic field of the eddy currents. In PEC profiling, this PEC signal is averaged over a fixed time interval after switching off the current in the transmission coil.

## The PEC profiling method

### *1.1 Principle of PEC Profiling*

The principle of PEC profiling is illustrated with Figure 2, and makes use of a transmitter and a receiver coil at a lift-off distance above an electrical conductor. The transmitter and receiver coils are housed in a PEC probe. The transmitter coil is energized with an electrical current that generates a primary magnetic field in the electrical conductor. The current is abruptly switched off, see Figure 2, thereby collapsing the primary magnetic field and thereby inducing eddy currents in the conductor. These eddy currents generate a secondary magnetic field that penetrates the receiver coil in the PEC probe. The eddy currents decay over time due to the electrical resistance of the conductor. As a result, the secondary magnetic field in the receiver coil changes, which in turn induces a voltage in the receiver coil. The induced voltage as a function of the time is referred to as the 'PEC signal' and can be recorded for analysis.

The objective of PEC profiling is to size external wall loss defects in metal samples, such as the one shown schematically in Figure 3. To this end, PEC signals are first recorded on a spot of a test sample away from the defect for several values of the lift-off between PEC probe and steel surface (Figure 3a). The strength of the PEC signal is averaged over a time interval. This time interval in the PEC signal is indicated in the voltage versus time graph in Figure 2 by two arrows. The signal strength is displayed in Figure 3b as a function of lift-off. This is the calibration curve. Next, PEC measurements are recorded on positions along a straight line with respect to the metal sample (Figure 3c). The PEC signal strength measured at these positions is compared with the calibration curve to determine the sensor lift-off for each sensor position. The graph of lift-off versus sensor position reflects the surface profile of the sample. Figure 3d displays an example of such a graph. The position and depth of the defect is apparent from the latter Figure.

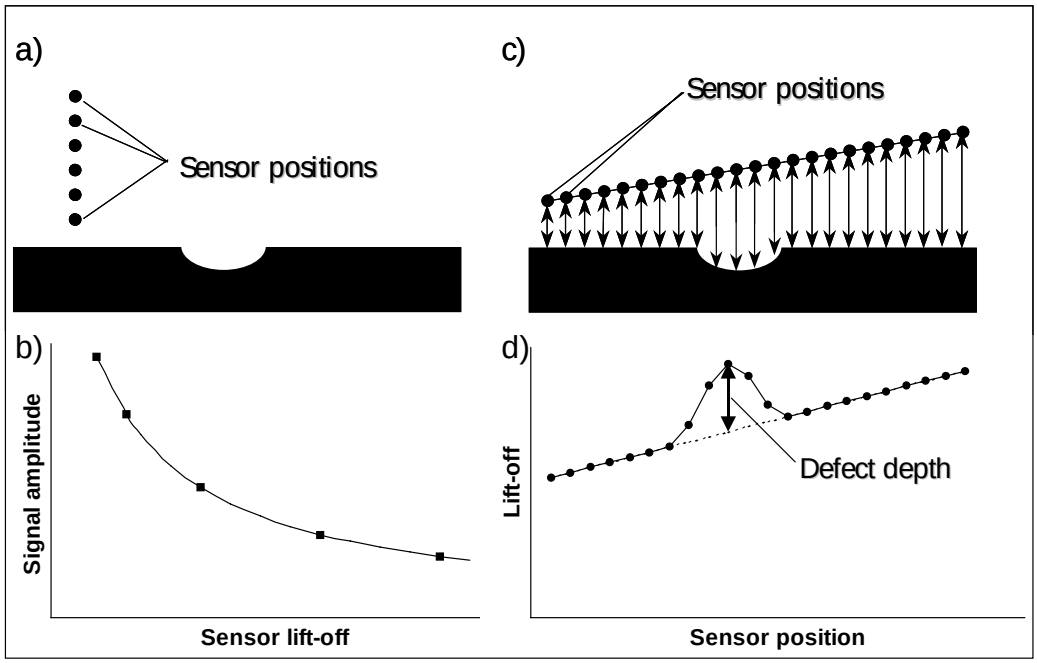


**Figure 3.** (a) Sensor positions used for calibration; (b) Calibration curve: Averaged PEC signal amplitude as a function of sensor lift-off; (c) Sensor positions for a measurement over an external defect; (d) lift-off profile measured over a defect. The position and depth of defect is deduced from this profile.

*1.2 Measurements*

To illustrate the method, PEC profiles have been recorded on the pipe sample displayed in Figure 1. The data were recorded along lines parallel to the pipe axis at several positions along the surface of the pipe. The remaining steel thickness was deduced from the profiles under the assumption that there is no internal corrosion. Figure 4 is a colour-coded representation of the remaining wall thickness. The colour coding emphasises differences in wall thickness and demonstrates that there is a band of severe corrosion. The data even indicate that there is a hole in the pipe (shown as a white cell in the colour plot), which was later confirmed by destructive examination of the pipe.

*1.3 Measurements through Corrosion Product*

The conductive and magnetic properties of paint, plastics, concrete, bitumen, air and virtually any other electrically insulating material are nearly equal to a vacuum. As a result, the PEC signal is virtually unaffected by the presence of any insulation layer between the coils and conductor. Corrosion products, i.e. iron oxides, on the other hand, have a relative magnetic permeability of typically $\mu_r \approx 200$ and need to be taken into account with the PEC profiler method. The influence of corrosion product is illustrated in Figure 5. This figure displays PEC signals recorded on a) only corrosion product, b) only steel and c) corrosion product on top of steel. For reasons of clarity, the PEC signals are presented on a double logarithmic axis. The PEC signal recorded on steel alone is approximately a straight line till about 10ms, which indicates that the decay rate in the log-signal versus log-time graph is roughly constant till 10ms. After that time, the decay of the PEC signal is much faster. The PEC signal recorded on the corrosion products alone decays at an even rate over the whole time domain.

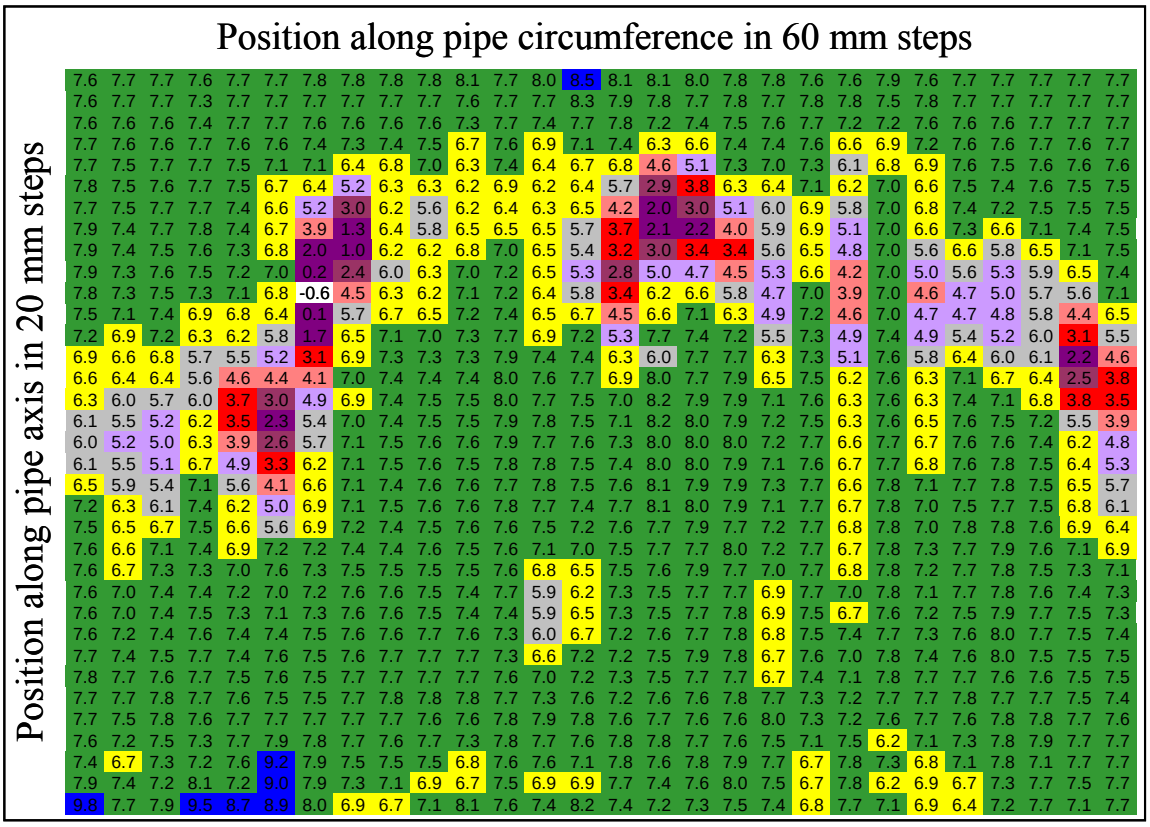


**Figure 4.** Colour-coded presentation of the remaining wall thickness [in mm] measured by PEC profiling on the pipe displayed in Figure 1. The spacing between sensor positions is 20 mm in the direction of the pipe and 60 mm in the direction along the circumference.

It is noted here that the conductivity of corrosion product is negligible compared to steel, so that there are no eddy currents in the corrosion product. Instead, the corrosion products demagnetise through thermal relaxation of the magnetic domain. Our experiments on a wide range of samples of corrosion product formed by steel under atmospheric conditions show that the shape of the PEC signals recorded on corrosion product is largely independent of thickness and constitution. The PEC signal recorded on corrosion product on top of steel is displayed in Figure 5. Careful examination of the signals shows that the signal is a good approximation to a linear combination of a PEC signal recorded on steel alone and a PEC signal recorded on corrosion products alone. Two time windows are shown in Figure 5: between about 3ms and 9ms (window 1) and between 60ms and 160ms after the excitation current was interrupted (window 2). The signal strength in the second window is dominated by the contribution of corrosion product; window 1 has contributions of both steel and corrosion product.

A calibration procedure has been developed to separate the distribution of the steel and corrosion product, based on the signal strength in both windows. The calibration procedure uses shims of corrosion products fixed in epoxy films. Calibration data with shims of different thickness are generated to be able to correct experimental PEC signals for the contribution of corrosion product. The method has been validated on defects that were first measured with corrosion product and a second time after the corrosion product had been removed.

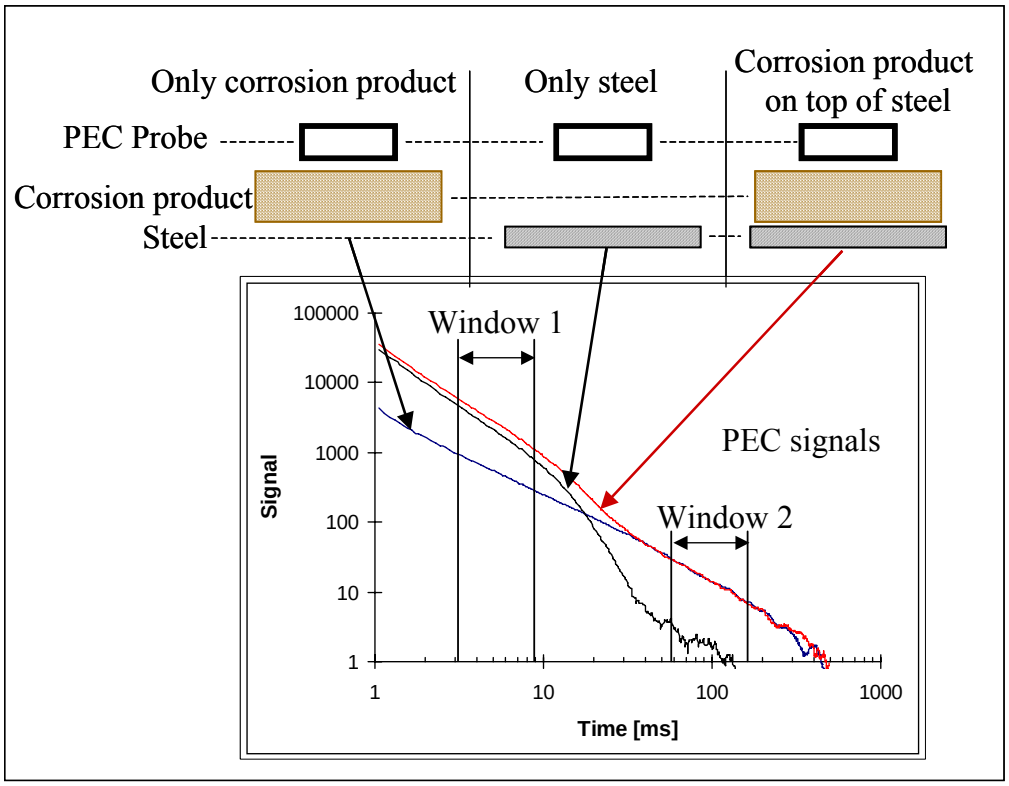


**Figure 5.** PEC signals recorded (a) on corrosion product alone, (b) on steel alone and (c) on corrosion product on top of steel. The contributions to the PEC signal of corrosion product and of steel are separated using two time windows in the PEC signal.

## 2. Finite element model calculations

### *2.1 Modelling of PEC Profiler*

In order to study the performance of the PEC profiler a model was developed. This model is an extension of the lumped circuit model created by Van den Berg in 2003 [2], to study the response of a one-dimensional array of stacked coils. We extended this work by modelling a three-dimensional system of concentrically stacked coils, displayed schematically in Figure 6. An additional single coil is placed above the coil stack. This single coil represents the transmitter and receiver coil; the coil stack models the conductor in which the eddy currents are induced. A wall loss defect is modelled by removing a number of coils from the stack. In Figure 6, for instance, 3 coils have been removed and these are hatched in the Figure. The present configuration is axially symmetric; it models a circular coil right above an axially symmetric wall loss defect. It is not intended for a configuration with non-circular transmitter and receiver coils nor for the situation in which the transmitter is off-centre from the wall loss defect.

The response of the coils is determined by their self- and mutual inductance and by the resistance of the coils. The current through each of these coils is described by the following system of homogeneous ordinary differential equations

$$\partial_t \mathbf{I} = -\mathbf{M}^{-1}\mathbf{R}\mathbf{I} \qquad (1)$$

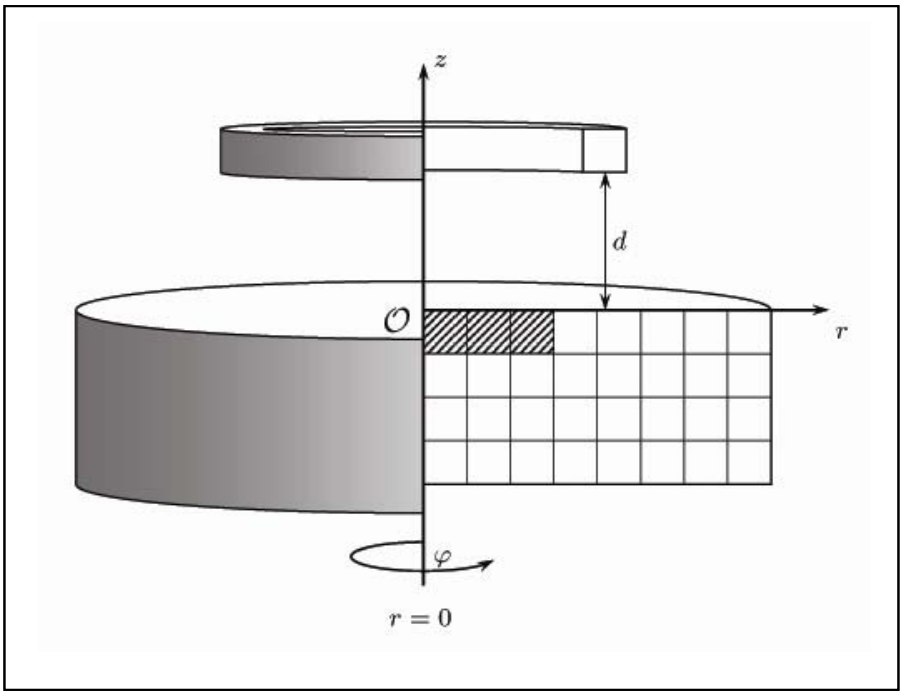


**Figure 6.** Configuration of concentric coils used for the modelling. The steel plate is modelled by concentric and stacked coils. The transmitter and receiver coils are represented by a single coil in vacuum at a distance d above the stacked coils.

In the literature no closed-form relationship can be found to calculate the self or mutual inductance of coils with inhomogeneous cores. Instead, the finite element simulation package FEMLAB of Comsol Multiphysics [4], [5] has been used to calculate the magnetic vector potential $\mathbf{A}_i$ due to a current $I_i$ through a coil *i*. Since we assumed cylindrical symmetry, the magnetic vector potential will have just one component $A_{\varphi,i}$. Next, the magnetic flux through each of the coils was determined from

$$\begin{aligned} \Phi_{m,j} &= \int_{S_j} \mathbf{B}\cdot \mathrm{d}\mathbf{S} = \int_{S_j} (\nabla\times\mathbf{A})\cdot \mathrm{d}\mathbf{S}, \\ &= \oint_{C_j} A_{\varphi,i}\, \mathrm{d}l = 2\pi R_j A_{\varphi,i}. \end{aligned} \qquad (2)$$

The self and mutual inductances were calculated from the magnetic flux using the relation

$$M_{ij} = \frac{\Phi_{m,j}}{I_i} = \frac{2\pi R_j A_{\varphi,i}}{I_i}. \qquad (3)$$

This determines all elements of the inductance matrix $\mathbf{M}$ of equation (1). Using these static inductances, the transient diffusive behaviour of the eddy currents is calculated solving equation (1) using eigenvalue analysis [3]. From this solution, the induced voltage in the receiving coils, i.e. the PEC signal, is found using

$$V_{\mathrm{PEC}} = V_1 = -\frac{\mathrm{d}\Phi_{m,1}}{\mathrm{d}t} = -\mathbf{M}_1\cdot\left(\frac{\mathrm{d}\mathbf{I}}{\mathrm{d}t}\right), \qquad (4)$$

where $\mathbf{M}_1$ is the first column of inductance matrix $\mathbf{M}$.

*2.2 Numerical Results*

Calculations have been carried out for a 15 mm thick steel plate with electrical conductivity $\sigma = 6.7\times10^6$ S/m and relative magnetic permeability $\mu_r = 200$. The diameter of the receiver/transmitter coil is 30 mm and its lift-off above the steel surface is 1 mm. There is a

cylindrical, flat-bottom hole with a 30 mm diameter and a depth of 4.5mm coaxial with the transmitter/receiver coil. Figure 7 displays a colour-coded spatial distribution of the eddy currents in the steel. It shows the current distribution in a cross section through the flat bottom hole at 0ms, 3ms, 40ms and 160ms after the excitation current has been switched off. The colour coding has been normalised for each moment in time separately. The location of the flat-bottom hole is indicated in Figure 7 as well.

At $t=0\,\text{ms}$, the eddy currents displayed in Figure 7 are concentrated at two spots near the steel surface: i.e. at the bottom of the hole and at the edge. These two current concentrations diffuse down and outward ($t=3\,\text{ms}$) and later merge into one concentration (see $t=40\,\text{ms}$ and $t=100\,\text{ms}$). It is observed that the eddy current distribution expands in the radial direction, like a 'smoke ring'. The radius of the centre of the eddy current distribution is approximately the same radius as the transmitter coil at $t=0\,\text{ms}$ but is twice as large at $t=100\,\text{ms}$. This implies that the best spatial resolution of the PEC profiler can be obtained by using in the analysis of the PEC signals a time window close to $t=0\,\text{ms}$, since in that case the area in which eddy current circulate is at its minimum.

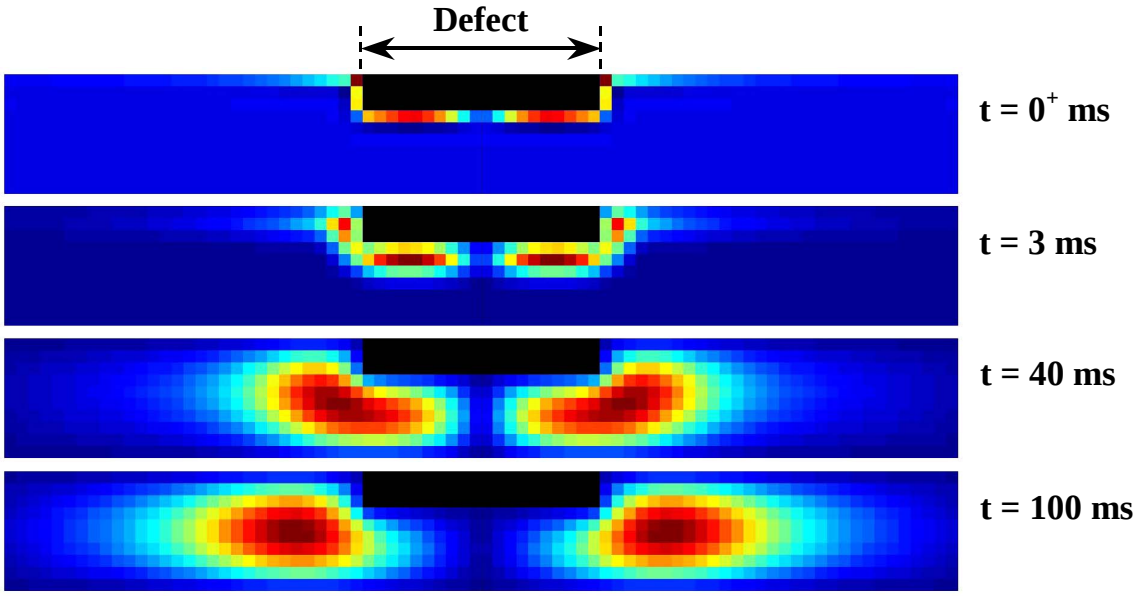


**Figure 7.** Calculated eddy current distribution for a 4.5 mm deep flat bottom hole with a diameter of 30 mm in a 15 mm thick steel plate calculated at 0ms, 3ms, 40ms and 100ms after the excitation current has been switched off. The colour coding has been normalised at each time separately. Blue is minimal amplitude; dark red is maximal amplitude.

The current distribution cannot be verified directly with experimental data, but the PEC signal can, at least qualitatively. Figure 8 displays the PEC signal obtained for the same parameters as used to calculate Figure 7. The signal obtained shows an approximately straight decay in the log-signal versus log-time diagram, with a slope of $\frac{d\log\left(V/V_0\right)}{d\log\left(t/t_0\right)}\approx -1.7$. At $t\approx 20\,\text{ms}$, the PEC signal starts to decay at an increasingly fast rate. This behaviour has been observed experimentally as well, in e.g. the PEC signal recorded on steel and displayed in Figure 5. It is therefore concluded that the model calculations, at least qualitatively, agree with measured PEC signals.

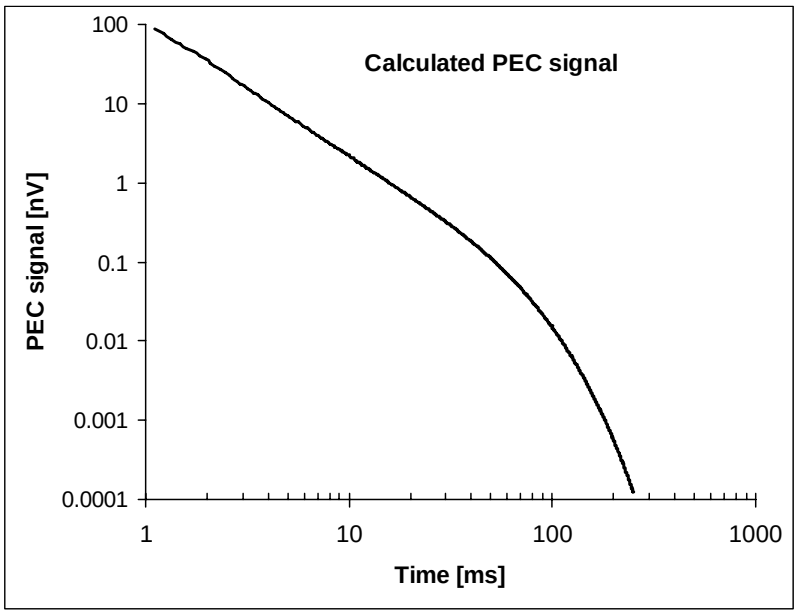


**Figure 8.** Calculated PEC signal for a 15 mm thick steel plate with electrical conductivity $\sigma = 6.7 \times 10^6$ S/m and relative magnetic permeability $\mu_r = 200$ with a 4.5mm deep, flat-bottom hole with a diameter of 30 mm.

The model calculations have been used to predict the ability of the PEC profiler to detect localised wall loss. To this end, PEC responses have been calculated as a function of defect diameter and defect depth. Figure 9 displays an example of the results, showing the defect depth determined by the profiler as a function of the actual defect depth for cylindrical flat bottom holes with a diameter of 30 mm. Both calculated and experimental results are displayed. The experimental results have been obtained with flat bottom holes machined in a 15.6 mm thick steel plate. There is a good agreement between measurements and model calculations; the largest relative deviation between measurement and calculation is less than 10%. Both measurements and model calculations underestimate the defect depth. The defect depth determined by the PEC profiler is for instance only 4.6 mm (measured) and 4.8 mm (calculated) at an actual defect depth of 6.5 mm, i.e., an under sizing by 29% and 26%, respectively. The model calculations have been used to determine the degree of under sizing as a function of defect depth and diameter. This shows that the discrepancy is negligible for large defects (i.e., about 50 mm diameter), but increases with decreasing defect diameter.

The difference between actual defect depth and PEC profiler measurements of small defects is attributed to the eddy currents that are induced around the edge of the defect, see Figure 7. As discussed above, there are two concentrations of eddy currents: one in the bottom of the defect and one at the edge of the defect. Only the former will lead to correct depth measurement by the PEC profiler. The eddy currents at the defect edge, on the other hand, are independent of the defect depth and will cause deviations between measured and actual defect depth.

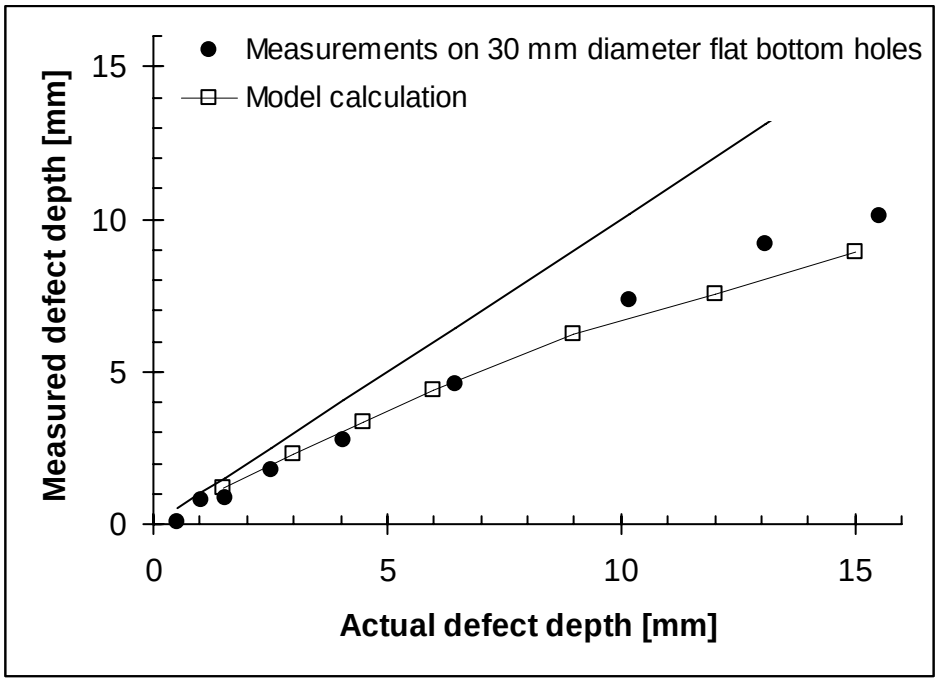


**Figure 9.** Depth determined by PEC profiling as a function of actual depth of a 30 mm diameter flat bottom hole defect in a 15.6 mm thick steel plate

## 3. Conclusions

A novel method has been presented to detect and size external corrosion damage using Pulsed Eddy Current Profiling. PEC profiling does not require the removal of corrosion product and can therefore be applied without any surface preparation. The method has therefore potential to assess external corrosion damage while the equipment remains in service. Model calculation and experiments show that the PEC profiler underestimates the defect depth by about 30% for defects with 30 mm diameter. The degree of under sizing is less for larger defects.

## References

[1] P.C.N. Crouzen, "Determining a surface profile of an object, International application number PCT/EP2003/002040, published 4 September 2003.
[2] Berg, S.M. van den, Modelling and Inversion of Pulsed Eddy Current Data, Laboratory of Electromagnetic Research, Delft University of Technology, The Netherlands, December, 2003.
[3] Lay, D.C., Linear Algebra and its Applications, Second Edition, Addison Wesley Longman Inc., ISBN 0-201-76717-1, United States of America, 1997.
[4] Comsol AB, FEMLAB Electromagnetics Module Manual, Comsol Multiphysics Modeling, FEMLAB 2.3, 3rd printing, Stockholm, Sweden, June, 2002.
[5] Comsol AB, FEMLAB Reference Manual, Comsol Multiphysics Modelling, FEMLAB 2.3a, 3rd printing, Stockholm, Sweden, January, 2003.